DOI: 10.3901/CJME.2010.03.367, available online at www.cjmenet.com; www.cjmenet.com.cn

Dynamic Modeling of a Roller Chain Drive System Considering the Flexibility of Input Shaft

XU Lixin[1], YANG Yuhu[1,*], CHANG Zongyu[2], and LIU Jianping[1]

1 *School of Mechanical Engineering, Tianjin University, Tianjin 300072, China*
2 *College of Engineering, Ocean University of China, Qingdao 266100, China*

Received June 16, 2009; revised February 5, 2010; accepted February 10, 2010; published electronically February 25, 2010

Abstract: Roller chain drives are widely used in various high-speed, high-load and power transmission applications, but their complex dynamic behavior is not well researched. Most studies were only focused on the analysis of the vibration of chain tight span, and in these models, many factors are neglected. In this paper, a mathematical model is developed to calculate the dynamic response of a roller chain drive working at constant or variable speed condition. In the model, the complete chain transmission with two sprockets and the necessary tight and slack spans is used. The effect of the flexibility of input shaft on dynamic response of the chain system is taken into account, as well as the elastic deformation in the chain, the inertial forces, the gravity and the torque on driven shaft. The nonlinear equations of movement are derived from using Lagrange equations and solved numerically. Given the center distance and the two initial position angles of teeth on driving and driven sprockets corresponding to the first seating roller on each side of the tight span, dynamics of any roller chain drive with two sprockets and two spans can be analyzed by the procedure. Finally, a numerical example is given and the validity of the procedure developed is demonstrated by analyzing the dynamic behavior of a typical roller chain drive. The model can well simulate the transverse and longitudinal vibration of the chain spans and the torsional vibration of the sprockets. This study can provide an effective method for the analysis of the dynamic characteristics of all the chain drive systems.

Key words: roller chain, dynamic modeling, Lagrange equations

1 Introduction

As an effective way of transmitting power, chain drives can be found extensively in nearly all mechanical engineering areas. The major advantages of chain drives are the flexibility in selecting shaft center, the ability to drive more than one shaft, the high reliability and durability. However, the application of chain drives introduces problems such as noise and vibration, which motivated researchers to investigate the dynamic behavior of them for various engineering purposes. For a comprehensive review on this subject, the reader is referred to WANG, et al[1].

For recent work, VEIKOS, et al[2-3], devised a realistic analytical procedure for the dynamic analysis of roller chain drives. Many test cases had been performed using this procedure with various types of chains, operating at different speeds, sprocket ratios and loads. CHOI, et al[4], developed a model based on axially moving material to study transverse vibration of roller chain drives. The chain span was approximated as rigid bar at low speeds and elastic bar at moderate or high speeds. In this model, the impact, polygonal action and external periodic load were considered. Then, a refined dynamic model of roller chain drive was developed by KIM, et al[5], the collisions and rebounds of the engaging roller were studied. The authors above all used the simplified model and have studied a sprocket and the tight side of the chain drive.

When the emphasis is on the system's global vibration and dynamic behavior, a complete chain transmission which regards the chain spans as two axially moving strings with their ends fixed to two rigid sprockets was developed by WANG[6]. In the subsequent work, LIU, et al[7], integrated the local meshing phenomena with the global chain/sprocket system dynamic behavior. In order to analyze the discrete nature of the chain spans in global chain/sprocket system, the chain strand was modeled as a series of individual lumped mass connected together by massless springs-damper[8-11]. The first to use the complete geometry with a dynamic model for determining the load distributions along the sprockets and the forces along the chain was TROEDSSON, et al[8-10]. In the model, the chain transmission was divided into four separate parts: the tight span, slack span, driving sprocket and driven sprocket, and each part was modeled and analyzed separately. Because the compatibility between the parts must be considered in a complete model, the boundary condition checking and solving procedure are complicated. A model of a roller

* Corresponding author. E-mail: yangyuhu@tju.edu.cn
This project is supported by National Natural Science Foundation of China (Grant No. 50605060), and Tianjin Municipal Science Foundation of China (Grant No. 06YFJMJC03300)

chain drive including the impact between the chain and guide-bars was developed by PEDERSEN, et al[11]. In the model, a real tooth profile is replaced by a circular tooth profile and the contacts between rollers and sprocket teeth are detected by kinematic constraints of using unilateral constraint methodology. Finite element techniques and numerical simulation software were used by ZHENG, et al[12], for predicting the meshing noise due to the impact of chain rollers against the sprocket of chain drives. In the model, the complete standard geometry of sprockets and all components of chain links were used with minor geometry simplification.

The objective in this study is to describe an automated, generally applicable computer procedure towards predictive design and analysis of the complete roller chain drives under dynamic conditions. A mathematical model is developed and the nonlinear equations of movement are derived from using Lagrange equations. The effect of the flexibility of input shaft on dynamic response of the chain system is taken into account, as well as the elastic deformation in the chain, the inertial forces, the gravity and the torque on driven shaft. A roller/sprocket tooth motion and contact detection analysis is described in detail in this study. Compared with the work made by TROEDSSON, et al[10], what is the simplest, no division is needed in the complete chain model and the boundary condition checking is easy. Dynamics of any roller chain drive with two sprockets and two spans can be analyzed by the procedure, if three necessary parameters, the center distance $\tilde{a}$ and the two initial position angles of teeth θ_1 and θ_2 on driving and driven sprockets corresponding to the first seating roller on each side of the tight span, are given. Finally, a numerical example is given and the procedure developed here is demonstrated by analyzing the dynamic behavior of a typical chain drive.

2 Dynamic Model

For purposes of analysis, the chain strand will be approximated as a series of point masses lumped at the roller centers which are connected together by massless springs-damper as used in theoretical works[8–11]. For simplifying complexity of the model, the following assumptions are made in the derivation of the chain equations of motion.

(1) All the links have equal mass, stiffness and undeformed pitch. One half of the total link mass is lumped at each roller.

(2) The rotational inertia of the rollers about their center of gravity is neglected.

(3) The chain pitch is equal to the sprocket pitch.

(4) All mechanical clearances are neglected.

(5) A real tooth profile is replaced by a circular tooth profile[11].

(6) The friction between the roller and the tooth flank in the part of the chain in contact with the sprocket is neglected.

(7) All parts of the model, both chain and sprockets are regarded as two dimensional bodies and all variations in the direction along the rotation axis of the sprockets are neglected.

Fig. 1 shows a model of a typical driving sprocket with chain links around it. A coordinate system is defined in the centre of the driving sprocket. This is the global coordinate system, used to describe the geometry, when calculating the position of the rollers and the sprockets. The position of any lumped mass point i can be expressed in x_i and y_i directions. The stretching forces in the two connecting links are called F_{i-1} and F_i. The contact force between the sprocket and the roller is called F_{ci} and the gravitation force is mg. Inertial forces in the chain, one in the radial direction $f_{sn} = mR_{s1}\dot{\varphi}_1^2$ and one in the tangential direction $f_{st} = mR_{s1}\ddot{\varphi}_1$, are considered since the rotation of sprockets is not at a nearly constant angular velocity. In these forces, the stretching forces and the contact force can be expressed as the spring-damping forces. Additionally, it is supposed that all the forces act at mass center. In the model, the input shaft is simplified as a torsion spring with constant torsional stiffness and damping. The constant or variable speeds boundary condition can be imposed on the rotation angle τ of input shaft. When the roller engages into the driven sprocket, its force condition is almost the same as it on driving sprocket. A torque M is imposed on the driven sprocket shaft in order to simulate the working load.

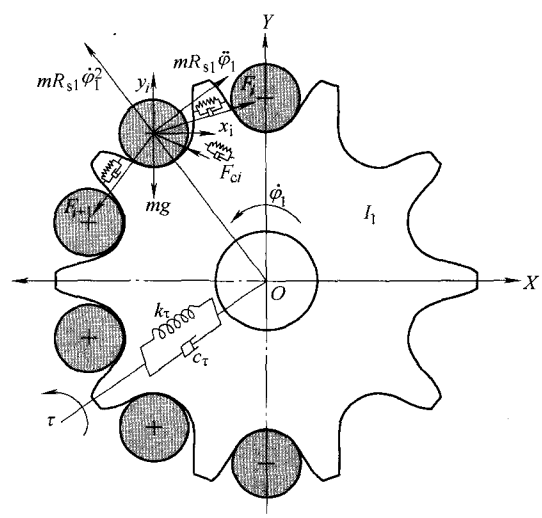

Fig. 1. Model of sprocket with the contacting chain part

Fig. 1 shows a standard geometry of sprocket tooth with three arcs and one straight line. Modeling the full sprocket geometry and detecting the contact between it and roller in movement is quite difficult. So, in this study a real tooth profile is replaced by a circular tooth profile as used in the work[11], as shown in Fig. 2. The advantage of this simplification is that the contacts between rollers and teeth can be determined easily. The radius of the circular tooth profile is R_t and the roller radius is R_r, yielding a clearance of $\Delta R = R_t - R_r$. In the engaging process, only

one single point at the tooth surface can simultaneously be in contact with the same roller.

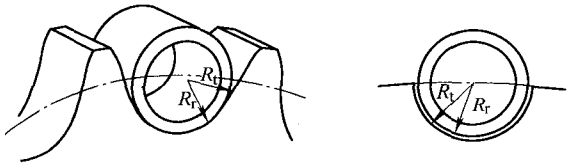

(a) Real tooth profile (b) Circular tooth profile

Fig. 2. Simplification of the tooth profile

The chain span is finally modeled as a series of mass points connected with massless spring elements as shown in Fig. 3. Both of the vibrations in x and y directions can be reflected by the model. The links in both the tight and the slack spans suffer the effect of gravity. In the movement, the engagement and disengagement phenomenon between rollers and sprocket teeth will occur periodically. The contact detection between them will be specified in next part: motion and contact detection analysis.

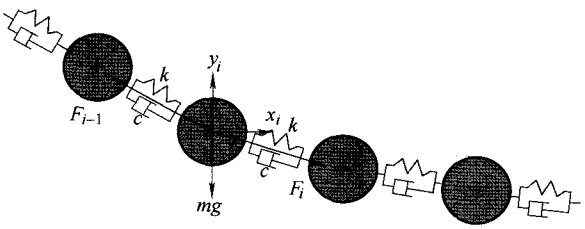

Fig. 3. Model of the chain span

3 Motion and Contact Detection Analysis

An example of a general chain transmission is shown in Fig. 4. It represents the simplest kind of transmission since it only includes two sprockets and one chain. One sprocket is driving, the other one is driven and the chain transmits the power between them. The two sprocket centers are assumed to be located at the same height with the gravitational force acting in the negative y direction.

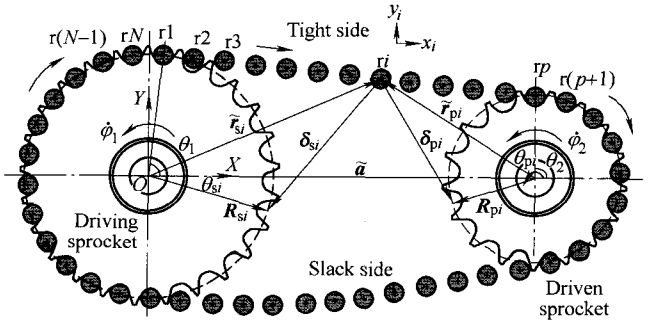

Fig. 4. Complete chain transmission in global coordinate system

To describe the model a few parameters have to be defined. As shown in Fig. 4, there are N links in the chain. The first link seated on the driving sprocket tooth will be indexed r1, along the arrow pointing direction, the number increase. It is assumed that the first link seated on the driven sprocket tooth will be indexed rp, and the last one in the chain is indexed rN ($1<p<N$). The initial position angles of teeth meshed with roller r1 and rp on driving and driven sprockets are defined θ_1 and θ_2 respectively. In the anticlockwise rotation of driving sprocket, the position angles of sprocket teeth corresponding to roller r1 and rp can be expressed as follows:

$$\theta_{s1} = \theta_1 + \varphi_1, \tag{1}$$

$$\theta_{p1} = \theta_2 + \varphi_2, \tag{2}$$

where φ_1 and φ_2 are the rotational angle of driving and driven sprockets, respectively. Then, the position angles of the correct seating teeth corresponding to roller ri on driving and driven sprockets can be derived from

$$\theta_{si} = \theta_1 + \varphi_1 - \frac{(i-1)\times 360^\circ}{z_1}, \tag{3}$$

$$\theta_{pi} = \theta_2 + \varphi_2 + \frac{(p-i)\times 360^\circ}{z_2}, \tag{4}$$

where z_1 and z_2 are numbers of teeth of driving and driven sprockets, respectively. In the movement, the deviation of roller ri from their correct seating positions on driving and driven sprockets denoted by $\boldsymbol{\delta}_{si}$ and $\boldsymbol{\delta}_{pi}$ are expressed as follows:

$$\boldsymbol{\delta}_{si} = \boldsymbol{R}_{si} - \tilde{\boldsymbol{r}}_{si}, \tag{5}$$

$$\boldsymbol{\delta}_{pi} = \boldsymbol{R}_{pi} - \tilde{\boldsymbol{r}}_{pi}, \tag{6}$$

which can be written as

$$\boldsymbol{\delta}_{si} = \begin{pmatrix} R_{s1}\cos\theta_{si} - x_i \\ R_{s1}\sin\theta_{si} - y_i \end{pmatrix}, \tag{7}$$

$$\boldsymbol{\delta}_{pi} = \begin{pmatrix} \tilde{a} + R_{s2}\cos\theta_{pi} - x_i \\ R_{s2}\sin\theta_{pi} - y_i \end{pmatrix}, \tag{8}$$

where R_{s1}, R_{s2} are the pitch radius for the driving and driven sprockets; $\tilde{a}$ is the center distance between the two sprockets. When the contact happens, two kinematic constraints are required to meet. For the contact between roller ri and the correct seating tooth on driving sprocket, the constraint is

$$\begin{cases} \|\boldsymbol{\delta}_{si}\| \geqslant R_t - R_r, \\ \|\tilde{\boldsymbol{r}}_{si}\| \leqslant R_{s1}. \end{cases} \tag{9}$$

For the contact between roller ri and its correct seating tooth on driven sprocket, the constraint is

$$\begin{cases} \left\| \boldsymbol{\delta}_{pi} \right\| \geqslant R_t - R_r, \\ \left\| \tilde{\boldsymbol{r}}_{pi} \right\| \leqslant R_{s2}. \end{cases} \tag{10}$$

Generally, the number of links in the chain is not an integral multiple of the number of sprocket teeth. Therefore, when the chain link r1 engages into the driving sprocket again, the seating tooth is not the previous one. At this point, in order to keep the correct meshing effects, the kinematic constraints between rollers and sprocket teeth need to be redefined. With the same case, when the chain link r*p* engages into the driven sprocket again, the kinematic constraints between rollers and sprocket teeth also need to be redefined.

4 Derivation of Equations of Motion

The equations of motion are derived from using Lagrange equations as

$$\frac{\mathrm{d}}{\mathrm{d}t}\left(\frac{\partial T}{\partial \dot{q}_i}\right) - \frac{\partial T}{\partial q_i} + \frac{\partial V}{\partial q_i} + \frac{\partial S}{\partial \dot{q}_i} = Q_i. \tag{11}$$

The derivation of the kinetic energy, deformation energy, dissipation function and generalized force of the system are shown in Appendix. Then the application of Lagrange equations leads to 2*N*+2 equations of motion. The equations of links in *x* and *y* directions are listed as follows:

$$\begin{aligned} & m\ddot{x}_i - k(x_{i-1} - x_i)\left[1 - \frac{l}{\sqrt{(x_{i-1} - x_i)^2 + (y_{i-1} - y_i)^2}}\right] + \\ & k(x_i - x_{i+1})\left[1 - \frac{l}{\sqrt{(x_i - x_{i+1})^2 + (y_i - y_{i+1})^2}}\right] - \\ & h_i k_c (R_{s1}\cos\theta_{si} - x_i) \times \\ & \left[1 - \frac{R_t - R_r}{\sqrt{(R_{s1}\cos\theta_{si} - x_i)^2 + (R_{s1}\sin\theta_{si} - y_i)^2}}\right] - \\ & q_i k_c (\tilde{a} + R_{s2}\cos\theta_{pi} - x_i) \times \\ & \left[1 - \frac{R_t - R_r}{\sqrt{(\tilde{a} + R_{s2}\cos\theta_{pi} - x_i)^2 + (R_{s2}\sin\theta_{pi} - y_i)^2}}\right] - \\ & c(\dot{x}_{i-1} - \dot{x}_i) + c(\dot{x}_i - \dot{x}_{i+1}) - h_i c_c[\dot{\varphi}_1 R_{s1}\cos(\theta_{si} + 90°) - \\ & \dot{x}_i] - q_i c_c[\dot{\varphi}_2 R_{s2} \times \cos(\theta_{pi} + 90°) - \dot{x}_i] = Q_{six} + Q_{pix}, \end{aligned} \tag{12}$$

$$\begin{aligned} & m\ddot{y}_i - k(y_{i-1} - y_i)\left[1 - \frac{l}{\sqrt{(x_{i-1} - x_i)^2 + (y_{i-1} - y_i)^2}}\right] + \\ & k(y_i - y_{i+1})\left[1 - \frac{l}{\sqrt{(x_i - x_{i+1})^2 + (y_i - y_{i+1})^2}}\right] - \\ & h_i k_c (R_{s1}\sin\theta_{si} - y_i) \times \\ & \left[1 - \frac{R_t - R_r}{\sqrt{(R_{s1}\cos\theta_{si} - x_i)^2 + (R_{s1}\sin\theta_{si} - y_i)^2}}\right] - \\ & q_i k_c (R_{s2}\sin\theta_{pi} - y_i) \times \\ & \left[1 - \frac{R_t - R_r}{\sqrt{(\tilde{a} + R_{s2}\cos\theta_{pi} - x_i)^2 + (R_{s2}\sin\theta_{pi} - y_i)^2}}\right] - \\ & c(\dot{y}_{i-1} - \dot{y}_i) + c(\dot{y}_i - \dot{y}_{i+1}) - h_i c_c[\dot{\varphi}_1 R_{s1}\sin(\theta_{si} + 90°) - \\ & \dot{y}_i] - q_i c_c \times [\dot{\varphi}_2 R_{s2}\sin(\theta_{pi} + 90°) - \dot{y}_i] + mg = Q_{siy} + Q_{piy}. \end{aligned} \tag{13}$$

The equations of motion of driving and driven sprockets are as follows:

$$\begin{aligned} & I_1\ddot{\varphi}_1 + \sum_{i=1}^{N} h_i k_c[-R_{s1}(R_{s1}\cos\theta_{si} - x_i)\sin\theta_{si} + \\ & R_{s1}(R_{s1}\sin\theta_{si} - y_i)\cos\theta_{si}] \times \\ & \left[1 - \frac{R_t - R_r}{\sqrt{(R_{s1}\cos\theta_{si} - x_i)^2 + (R_{s1}\sin\theta_{si} - y_i)^2}}\right] + \\ & \sum_{i=1}^{N}\{h_i c_c\{-\dot{\varphi}_1 R_{s1}[\dot{\varphi}_1 R_{s1}\cos(\theta_{si} + 90°) - \dot{x}_i] \times \\ & \sin(\theta_{si} + 90°) + \dot{\varphi}_1 R_{s1}[\dot{\varphi}_1 R_{s1}\sin(\theta_{si} + 90°) - \dot{y}_i] \times \\ & \cos(\theta_{si} + 90°)\}\} - k_\tau(\tau - \varphi_1) - c_\tau(\dot{\tau} - \dot{\varphi}_1) = 0, \end{aligned} \tag{14}$$

$$\begin{aligned} & I_2\ddot{\varphi}_2 + \sum_{i=1}^{N} q_i k_c[-R_{s2}(\tilde{a} + R_{s2}\cos\theta_{pi} - x_i)\sin\theta_{pi} + \\ & R_{s2}(R_{s2}\sin\theta_{pi} - y_i)\cos\theta_{pi}] \times \\ & \left[1 - \frac{R_t - R_r}{\sqrt{(\tilde{a} + R_{s2}\cos\theta_{pi} - x_i)^2 + (R_{s2}\sin\theta_{pi} - y_i)^2}}\right] + \\ & \sum_{i=1}^{N}\{q_i c_c\{-\dot{\varphi}_2 R_{s2}[\dot{\varphi}_2 R_{s2}\cos(\theta_{pi} + 90°) - \dot{x}_i] \times \\ & \sin(\theta_{pi} + 90°) + \dot{\varphi}_2 R_{s2}[\dot{\varphi}_2 R_{s2}\sin(\theta_{pi} + 90°) - \dot{y}_i] \times \\ & \cos(\theta_{pi} + 90°)\}\} = M. \end{aligned} \tag{15}$$

Where l is the undeformed chain link pitch; k and c are the longitudinal tensile stiffness of a chain link and the damping in the link respectively; k_c and c_c are the contact stiffness and contact damping respectively. In the equations, $i=1, 2, \cdots, N$, and it should be pay attention that $x_0 = x_N$, $y_0 = y_N$ when $i=1$. The Runge-Kutta-Fehlman(RKF) method is used for the resolution of equations of motion. The numerical method uses a variable-step-length algorithm to find the solution for a given ordinary differential equation. The contacts between rollers and sprockets then have to be calculated for every time step. Without contact (do not meet the requirement of Eqs. (9) or (10)), h_i or $q_i = 0$ and with contact (meet the requirement of formulas 9 or 10), h_i or $q_i = 1$.

5 Calculation of the Equivalent Contact Stiffness

For getting an accurate simulation results, the equivalent contact stiffness must be given reasonably. As shown in Fig. 5, since a link is an assembly of several components, the contact effect can be described as a pin-bush-roller assembly contact with the tooth surface. The equivalent contact stiffness can be seen as a series connection of the three contact stiffness. They are the contact between pin and bush (k_{pb}), contact between bush and roller (k_{br}) and contact between roller and tooth surface (k_{rt}). The contact between each other can be regarded as the contact between the parallel cylinder and the concave cylindrical surface under the load condition. According to the Hertz contact theory used in the Ref. [13], the contact stiffness between each other can be determined. Then the equivalent contact stiffness k_c can be given by

$$\frac{1}{k_c} = \frac{1}{k_{pb}} + \frac{1}{k_{br}} + \frac{1}{k_{rt}}. \tag{16}$$

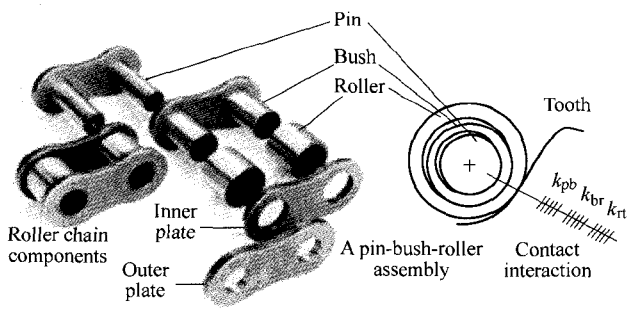

Fig. 5. Contact between pin-bush-roller assembly and sprocket tooth

6 Calculation of the Longitudinal Tensile Stiffness of a Chain Link

In the longitudinal direction of the chain, only the elastic deformation of the link plates is considered. The finite element method was used to calculate the stiffness in the link in the study[8]. In this work, a comparatively accurate experimental method is used to calculate the longitudinal tensile stiffness of a link. Fig. 6 shows the experimental apparatus and testing result. By drawing the chain, the elongation of a link plate is measured by a deformation sensor. The stiffness k can be calculated by the relationship between force and deformation. A chain is normally made by two kinds of link pair, which is one outer pair and one inner pair. The outer pair is normally smaller than the inner pair. The stiffness for one outer and one inner was tested and the mean value was then used in the model.

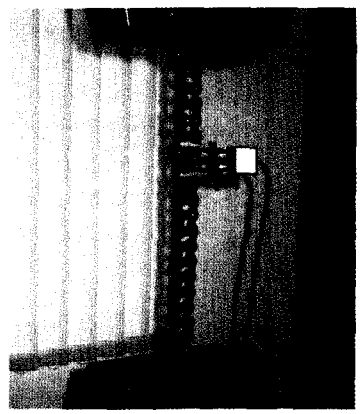

(a) Experimental apparatus

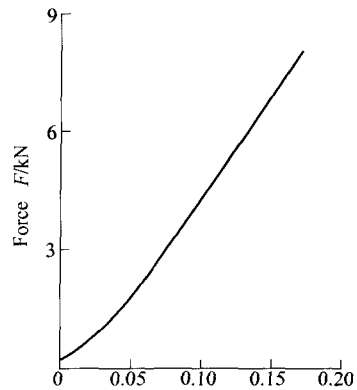

(b) Testing result

Fig. 6. Stiffness calculation for a chain link

7 Numerical Example

A roller chain drive system, which has the number of chain links $N=40$, sprocket teeth $z_1=20$ and $z_2=10$, was taken as an example[10]. Here, the studied chain drive system has the number of chain links $N=46$, the sprocket teeth $z_1=25$ and $z_2=17$, the center distance $\tilde{a}=197.7$ mm (see Fig. 4). The sprockets and the chain links have the same pitch $l=15.875$ mm. Compared with the 20/10 sprocket teeth model, the advantage of this numerical example is that it meets the requirement of the smallest tooth number of the small sprocket under the condition of pitch $l=15.875$ mm according to the engineering

application background. The example can be able to reflect the general characteristics of a roller chain drive. The torsional stiffness for input shaft k_t =12 kN • m • rad^{-1}, the mass of a chain link including one roller m=0.016 2 kg, the equival ent contact stiffness is 8.46 kN/mm, a mean value of the longitudinal tensile stiffness of a chain link is 51 kN/mm, the moments of inertia for the driving and driven sprockets I_1=4 010.8 kg • mm^2 and I_2=933 kg • mm^2 and the torque M on driven shaft is 43.2 kN • mm. An accurate calculation of damping is quite difficult. However, damping must be introduced to produce a stable solution. In the numerical example, the damping in the chain is 100 N • s • m^{-1}. In simulation, the speed of input shaft is 120 r/min. The angular velocity of input shaft starts at zero, after 0.05 s it reaches 120 r/min. Then the initial velocities of chain links and the initial angular velocities of driving and driven sprockets can be taken zero.

Fig. 7 shows the tension force in chain spans, one in the tight span and one in the slack span. It can be found that the tight span bears a lager load. Before the link engages into the driving sprocket, the magnitude of the tension force reaches the maximum value and its fluctuation is also serious. This is caused by the fact that, due to the polygon action and the impact between roller and tooth, the force in the connecting link at the tight span on the driving sprocket increases. This simulation result is in agreement with the result made by TROEDSSON, et al[10].

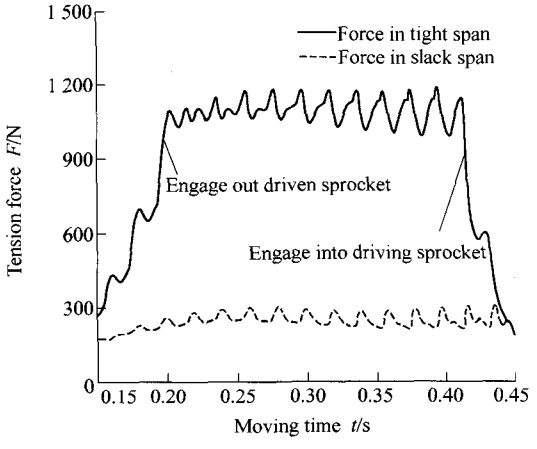

Fig. 7. Tension force in chain spans

Fig. 8 shows the vibration of a chain link in tight span in x and y directions, respectively. The link engages out the driven sprocket and moves toward the driving sprocket. In this movement, it is interesting to notice that most of the vibration comes from the impact when a roller comes into contact with the driving sprocket.

Fig. 9 shows the vibration of a chain link in slack span in x and y directions, respectively. The link engages out the driving sprocket and moves toward the driven sprocket. Compared with the vibration of the link in tight span, it is observed that the vibration of slack span is relatively small. In the slack span, when the link approaches the driven sprocket, the vibration strengthens gradually.

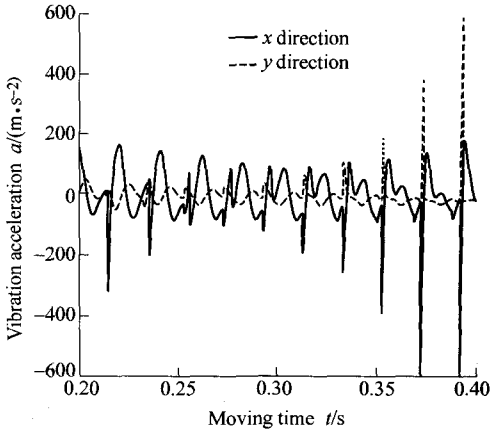

Fig. 8. Vibration of a chain link in tight span

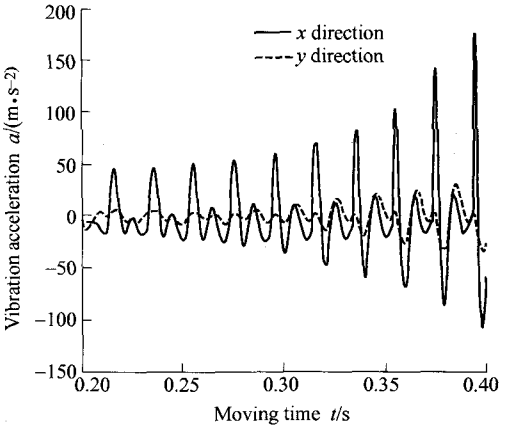

Fig. 9. Vibration of a chain link in slack span

The torsional vibration of the driving and driven sprockets is shown in Fig. 10, including the time-domain vibration response and their frequency analysis. It is observed that the fundamental frequency of excitation is the meshing frequency 50 Hz. In addition to the basic frequency, harmonic components still exist. In the simulation, it is found that the torsional vibration of driving sprocket is relatively larger than that of driven sprocket. This is caused by the fact that the input shaft is not rigid and the driving sprocket bears the impact and larger tension force in tight span. With the increase of torsional stiffness of input shaft, the vibration of driving sprocket will be weakened.

8 Conclusions

(1) A dynamic model of a complete roller chain drive system considering the flexibility of input shaft is developed. Dynamics of any roller chain drive with two sprockets and two spans can be analyzed by the procedure if the center distance and the initial position angles of teeth on driving and driven sprockets corresponding to the first seating roller on each side of the tight span are given.

(2) The most vibrations of the chain spans, the increased tension force in tight span and its fluctuation are mainly caused by the meshing impact between roller and sprocket

tooth.

(3) When the flexibility of the input shaft is taken into account, the effect of meshing impact on the vibration of driving sprocket is greater than it on the vibration of driven sprocket. With the increase of torsional stiffness of input shaft, the vibration of driving sprocket will be weakened.

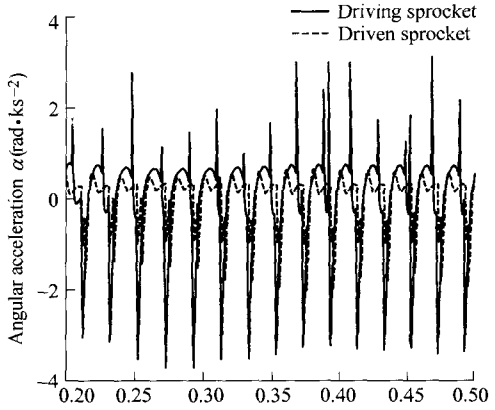

(a) Time domain response

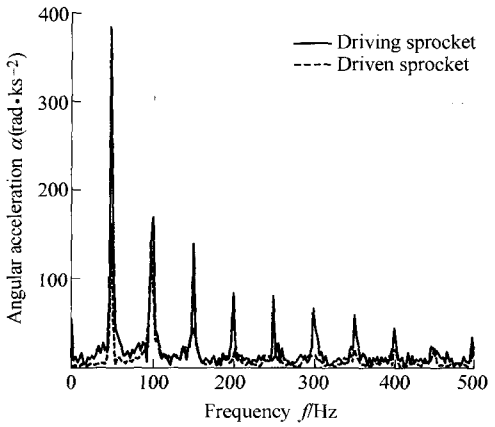

(b) Frequency domain analysis

Fig. 10. Vibration of driving and driven sprockets

References

[1] WANG K M, LIU S P. On the noise and vibration of chain drive systems[J]. *Shock and Vibration Digest*, 1991, 23(4): 8–13.

[2] VEIKOS N M, FREUDENSTEIN F. On the dynamic analysis of roller chain drives: part 1-theory[C]//*Proceedings of the 22nd Biennial Mechanisms Conference*, Scottsdale, AZ, USA, September 13–16, 1992: 431–439.

[3] VEIKOS N M, FREUDENSTEIN F. On the dynamic analysis of roller chain drives: part II-case study[C]//*Proceedings of the 22nd Biennial Mechanisms Conference*, Scottsdale, AZ, USA, September 13–16, 1992: 441–450.

[4] CHOI W, JOHNSON G E. Vibration of roller chain drives at low, medium and high operating speeds[C]//*Proceedings of the 14th Biennial ASME Conference on Vibration and Noise*, Albuquerque, NM, USA, September 19–22, 1993: 29–40.

[5] KIM M S, JOHNSON G E. General, multi-body dynamic model to predict the behavior of roller chain drives at moderate and high speeds[C]//*Proceedings of the 14th Biennial Conference on Mechanical Vibration and Noise*, Albuquerque, NM, USA, September 19–22, 1993: 247–468.

[6] WANG K W. On the stability of chain drive systems under periodic sprocket oscillations[J]. *Journal of Vibration and Acoustics*, 1992, 114(1): 119–126.

[7] LIU S P, WANG K W, HAYEK S I, et al. A global-local integrated study of roller chain meshing dynamics[J]. *Journal of Sound and Vibration*, 1997, 203(1): 41–62.

[8] TROEDSSON I, VEDMAR L. A method to determine the static load distribution in a chain drive[J]. *Journal of Mechanical Design*, 1999, 121(3): 402–408.

[9] TROEDSSON I, VEDMAR L. A method to determine the dynamic load distribution in a chain drive[J]. *Journal of Mechanical Engineering Science*, 2001, 215(5): 569–579.

[10] TROEDSSON I, VEDMAR L. A dynamic analysis of the oscillations in a chain drive[J]. *Journal of Mechanical Design*, 2001, 123(3): 395–401.

[11] PEDERSEN S L, HANSEN J M, AMBROSIO Jorge A C. A roller chain drive model including contact with guide-bars[J]. *Multibody System Dynamics*, 2004, 12(3): 285–301.

[12] ZHENG H, WANG Y Y, LIU G R, et al. Efficient modeling and prediction of meshing noise from chain drives[J]. *Journal of Sound and Vibration*, 2001, 245(1): 133–150.

[13] ZOU H J. *Modern design of cam mechanism*[M]. Shanghai: Shanghai Jiao Tong University Press, 1991. (in Chinese)

Biographical notes

XU Lixin, born in 1982, is currently a PhD candidate in School of Mechanical Engineering, Tianjin University, China. He obtained his master degree from Tianjin University in 2008. His research interests include structural dynamics, multi-body dynamics and the elastic dynamics of high speed mechanical systems.
Tel: +86-22-27404071; E-mail: xulixin_tju@yahoo.cn

YANG Yuhu, born in 1962, is currently a professor in School of Mechanical Engineering, Tianjin University, China. His research interests include mechanism and machine theory.
Tel: +86-22-27404071; E-mail: yangyuhu@tju.edu.cn

CHANG Zongyu, born in 1973, is currently a professor in College of Engineering, Ocean University of China. His research interests include mechanism and machine theory.
E-mail: zongyuchang@yahoo.com.cn

LIU Jianping, born in 1953, is currently a professor in School of Mechanical Engineering, Tianjin University, China. His research interests include mechanism and machine theory.
E-mail: liujianping@tju.edu.cn

Appendix

The total kinetic energy of the system is

$$T=\frac{1}{2}\sum_{i=1}^{N}m_i(\dot{x}_i^2+\dot{y}_i^2)+\frac{1}{2}I_1\dot{\varphi}_1^2+\frac{1}{2}I_2\dot{\varphi}_2^2. \tag{1}$$

The total energy of deformation is

$$U=\frac{1}{2}\sum_{i=1}^{N}k\left\{\left[(x_{i-1}-x_i)^2+(y_{i-1}-y_i)^2\right]^{\frac{1}{2}}-l\right\}^2+$$

$$\frac{1}{2}\sum_{i=1}^{N}h_ik_c\left\{\left\{\left\{R_{s1}\cos\left[\theta_1+\varphi_1-\frac{(i-1)\times 360^\circ}{z_1}\right]-x_i\right\}^2+\right.\right.$$

$$\left\{R_{s1}\sin\left[\theta_1+\varphi_1-\frac{(i-1)\times 360^\circ}{z_1}\right]-y_i\right\}^2\Bigg\}^{\frac{1}{2}}-(R_t-R_r)\Bigg\}^2+\frac{1}{2}\sum_{i=1}^{N}q_i k_c\times$$

$$\left\{\left\{\left\{\tilde{a}+R_{s2}\cos\left[\theta_2+\varphi_2+\frac{(p-i)\times 360^\circ}{z_2}\right]-x_i\right\}^2+\left\{R_{s2}\sin\left[\theta_2+\varphi_2+\frac{(p-i)\times 360^\circ}{z_2}\right]-y_i\right\}^2\right\}^{\frac{1}{2}}-(R_t-R_r)\right\}^2+\sum_{i=1}^{N}m_i g(y_i-0)+\frac{1}{2}k_\tau(\tau-\varphi_1)^2. \quad (2)$$

The dissipative energy in the chain system is

$$S=\frac{1}{2}\sum_{i=1}^{N}c\left[(\dot{x}_{i-1}-\dot{x}_i)^2+(\dot{y}_{i-1}-\dot{y}_i)^2\right]+\frac{1}{2}\sum_{i=1}^{N}h_i c_c\times\left\{\left\{\dot{\varphi}_1 R_{s1}\cos\left[\theta_1+\varphi_1-\frac{(i-1)\times 360^\circ}{z_1}+90^\circ\right]-\dot{x}_i\right\}^2+\left\{\dot{\varphi}_1 R_{s1}\sin\left[\theta_1+\varphi_1-\frac{(i-1)\times 360^\circ}{z_1}+90^\circ\right]-\dot{y}_i\right\}^2\right\}+$$

$$\frac{1}{2}\sum_{i=1}^{N}q_i c_c\left\{\left\{\dot{\varphi}_2 R_{s2}\cos\left[\theta_2+\varphi_2+\frac{(p-i)\times 360^\circ}{z_2}+90^\circ\right]-\dot{x}_i\right\}^2+\left\{\dot{\varphi}_2 R_{s2}\sin\left[\theta_2+\varphi_2+\frac{(p-i)\times 360^\circ}{z_2}+90^\circ\right]-\dot{y}_i\right\}^2\right\}+\frac{1}{2}c_\tau(\dot{\tau}-\dot{\varphi}_1)^2. \quad (3)$$

The generalized force acting at roller i on driving sprocket in x and y directions can be expressed as follows:

$$Q_{six}=h_i[f_{sn}\cos\theta_{si}+f_{st}\cos(\theta_{si}-90^\circ)], \quad (4)$$

$$Q_{siy}=h_i[f_{sn}\sin\theta_{si}+f_{st}\sin(\theta_{si}-90^\circ)]. \quad (5)$$

The generalized force acting at roller i on driven sprocket in x and y directions can be expressed as follows:

$$Q_{pix}=q_i[f_{pn}\cos\theta_{pi}+f_{pt}\cos(\theta_{pi}-90^\circ)], \quad (6)$$

$$Q_{piy}=q_i[f_{pn}\sin\theta_{pi}+f_{pt}\sin(\theta_{pi}-90^\circ)]. \quad (7)$$

Additionally, the generalized force on driven sprocket is the torque M.